

RESEARCH ARTICLE

Mitochondrial modulation-induced activation of vagal sensory neuronal subsets by antimycin A, but not CCCP or rotenone, correlates with mitochondrial superoxide production

Katherine R. Stanford, Thomas E. Taylor-Clark*

Department of Molecular Pharmacology & Physiology, Morsani College of Medicine, University of South Florida, Tampa, FL, United States of America

* ttaylorc@health.usf.edu



OPEN ACCESS

Citation: Stanford KR, Taylor-Clark TE (2018) Mitochondrial modulation-induced activation of vagal sensory neuronal subsets by antimycin A, but not CCCP or rotenone, correlates with mitochondrial superoxide production. PLoS ONE 13(5): e0197106. <https://doi.org/10.1371/journal.pone.0197106>

Editor: Agustín Guerrero-Hernandez, Cinvestav-IPN, MEXICO

Received: January 11, 2018

Accepted: April 26, 2018

Published: May 7, 2018

Copyright: © 2018 Stanford, Taylor-Clark. This is an open access article distributed under the terms of the [Creative Commons Attribution License](https://creativecommons.org/licenses/by/4.0/), which permits unrestricted use, distribution, and reproduction in any medium, provided the original author and source are credited.

Data Availability Statement: All relevant data are within the paper and its Supporting Information files.

Funding: This manuscript, and the work performed during its creation, was entirely funded by the National Heart Lung and Blood Institute (R01HL119802; PI: Taylor-Clark). The funders had no role in study design, data collection and analysis, decision to publish, or preparation of the manuscript.

Abstract

Inflammation causes nociceptive sensory neuron activation, evoking debilitating symptoms and reflexes. Inflammatory signaling pathways are capable of modulating mitochondrial function, resulting in reactive oxygen species (ROS) production, mitochondrial depolarization and calcium release. Previously we showed that mitochondrial modulation with antimycin A, a complex III inhibitor, selectively stimulated nociceptive bronchopulmonary C-fibers via the activation of transient receptor potential (TRP) ankyrin 1 (A1) and vanilloid 1 (V1) cation channels. TRPA1 is ROS-sensitive, but there is little evidence that TRPV1 is activated by ROS. Here, we used dual imaging of dissociated vagal neurons to investigate the correlation of mitochondrial superoxide production (mitoSOX) or mitochondrial depolarization (JC-1) with cytosolic calcium (Fura-2AM), following mitochondrial modulation by antimycin A, rotenone (complex I inhibitor) and carbonyl cyanide m-chlorophenyl hydrazone (CCCP, mitochondrial uncoupling agent). Mitochondrial modulation by all agents selectively increased cytosolic calcium in a subset of TRPA1/TRPV1-expressing (A1/V1+) neurons. There was a significant correlation between antimycin A-induced calcium responses and mitochondrial superoxide in wild-type ‘responding’ A1/V1+ neurons, which was eliminated in TRPA1^{-/-} neurons, but not TRPV1^{-/-} neurons. Nevertheless, antimycin A-induced superoxide production did not always increase calcium in A1/V1+ neurons, suggesting a critical role of an unknown factor. CCCP caused both superoxide production and mitochondrial depolarization but neither correlated with calcium fluxes in A1/V1+ neurons. Rotenone-induced calcium responses in ‘responding’ A1/V1+ neurons correlated with mitochondrial depolarization but not superoxide production. Our data are consistent with the hypothesis that mitochondrial dysfunction causes calcium fluxes in a subset of A1/V1+ neurons via ROS-dependent and ROS-independent mechanisms.

Competing interests: The authors have declared that no competing interests exist.

Abbreviations: AITC, allyl isothiocyanate; $[Ca^{2+}]_i$, intracellular calcium concentration; CCCP, carbonyl cyanide m-chlorophenyl hydrazine; JC-1, 5,5',6,6'-Tetrachloro-1,1',3,3'-tetraethylimidacarbocyanine iodide; mETC, mitochondrial electron transport chain; ROS, reactive oxygen species; TRPA1, transient receptor potential ankyrin 1; TRPV1, transient receptor potential vanilloid 1.

1. Introduction

The activation of nociceptive sensory nerves by noxious stimuli evokes defensive reflexes and pain, which serves to protect the body from further damage. Inflammation, infection, physical damage and exogenous irritants are capable of significant nociceptor activation. As such, excessive activation of this sensory subpopulation contributes to a wide-range of disease states including chronic pain, irritable bowel disease, colitis, arthritis and asthma [1,2]. Nociceptive sensory nerves are selectively activated by noxious stimuli due to their expression of a variety of receptors, including the allyl isothiocyanate (AITC)-sensitive transient receptor potential (TRP) ankyrin 1 (A1) channel and the capsaicin-sensitive TRP vanilloid 1 (TRPV1) channel [3,4]. Both TRPA1 and TRPV1 are nonspecific cation channels whose activation causes neuronal depolarization and action potential discharge. TRPV1 is expressed on the majority of nociceptive neurons [5–7], although it should be noted that some specific subsets of nociceptive A δ - and C-fiber nociceptors lack TRPV1 [8–10]. TRPA1 is expressed on approximately 66% of TRPV1-expressing neurons and <10% of neurons lacking TRPV1 expression [5–7,11,12]. TRPA1 is activated by a wide variety of electrophilic compounds, including reactive oxygen species (ROS) and environmental pollutants [13–16]. TRPV1 is activated directly by capsaicin, extracellular protons and heat, and indirectly downstream of second messenger signaling [3,17].

One potential way in which inflammation may cause nociceptor activation is by inducing the dysfunction of mitochondria, which are densely packed within sensory nerve terminals [18,19]. Mitochondrial dysfunction encompasses events including morphology changes, ROS production, mitochondrial depolarization and calcium release. While catastrophic mitochondrial dysfunction induces apoptosis, mitochondrial dysfunction also initiates signaling events involved in cellular stress responses. Chronic inflammation induces changes in mitochondrial morphology associated with dysfunction [20], and there are reports of an increased rate of mitochondrial DNA mutations and altered activity of ROS scavengers such as glutathione and superoxide dismutase in inflammatory states [21–23]. Inflammatory signaling has been shown to directly inhibit complexes I, II, and IV of the mitochondrial electron transport chain (mETC), resulting in ROS production and mitochondrial depolarization [24–27].

We have previously demonstrated that mitochondrial dysfunction induced by antimycin A, an mETC complex III inhibitor, activates vagal sensory neurons and bronchopulmonary C-fibers via the gating of TRPA1 and TRPV1 [28]. Inhibition of complex III by antimycin A induces ROS production and mitochondrial depolarization [29,30], but the role of these events in mitochondrial dysfunction-induced neuronal activation has not been established. Here we investigated the influence of mitochondrial dysfunction on the activation of vagal sensory neurons using three mitochondrial agents: antimycin A, carbonyl cyanide m-chlorophenyl hydrazine (CCCP, mitochondrial uncoupling agent), and rotenone (mETC complex I inhibitor). Using live cell co-imaging, we simultaneously monitored cytosolic calcium (as a surrogate for neuronal activation) and either mitochondrial superoxide production or changes in mitochondrial polarization. We found that the three agents activated (i.e. caused significant calcium fluxes) only a subset of A1/V1+ neurons, yet there was no difference in mitochondrial superoxide production or mitochondrial depolarization between 'responding' and 'non-responding' A1/V1+ neurons. Nevertheless, we observed a significant correlation between antimycin A-induced calcium responses and mitochondrial superoxide production in wild-type 'responding' A1/V1+ neurons, which was eliminated in TRPA1^{-/-} neurons, but not TRPV1^{-/-} neurons. CCCP-induced calcium responses did not correlate with either superoxide production or mitochondrial depolarization. Rotenone-induced calcium responses correlated with mitochondrial depolarization but not superoxide production. Our data are consistent with the

hypothesis that mitochondrial dysfunction causes the activation of a subset of A1/V1+ neurons via ROS-dependent and ROS-independent mechanisms.

2. Experimental procedures

2.1 Mouse models

Female TRPV1^{-/-} mice were mated with male TRPV1^{-/-} mice. Female TRPA1^{-/-} mice were mated with male TRPA1^{+/-} mice. Genotype of the offspring was confirmed using polymerase chain reaction. Wild type C57BL/6J mice were purchased from The Jackson Laboratory. All experiments were performed with approval from the University of South Florida Institutional Animal Care and Use Committee (AAALAC #000434).

2.2 Neuronal dissociation

Male 6–12-week-old mice were euthanized by CO₂ asphyxiation followed by exsanguination. Vagal ganglia were isolated followed by an enzymatic and mechanic dissociation then individual neurons were plated onto poly-D-lysine and laminin coated coverslips as previously described [28]. Neurons were incubated at 37°C in antibiotic-free L-15 media supplemented with 10% fetal bovine serum and used within 24 hours.

2.3 Live cell imaging

Cells were loaded with 4μM Fura-2AM for 45–60 minutes at 37°C. During the last 15 minutes of incubation, 2μM 5,5',6,6'-Tetrachloro-1,1',3,3'-tetraethyl-imidacarbocyanine iodide (JC-1), or 5μM MitoSOX Red was added in some studies. Coverslips were loaded into a chamber and perfused with heated (33–34°C) 10mM HEPES buffer (154mM NaCl, 4.7mM KCl, 1.2mM MgCl₂, 2.5mM CaCl₂, 5.6mM D-glucose). All drugs were diluted in HEPES buffer. Concentrations of mitochondrial modulators (antimycin A, 10μM; CCCP, 10μM; rotenone, 5μM) which induce acute mitochondrial ROS production and mitochondrial depolarization without significantly effecting cellular viability were used [31]. The vehicle (dimethyl sulfoxide (DMSO), 0.1%) for these experiments was the highest concentration of DMSO used in the dilution of mitochondrial inhibitor stocks into HEPES buffer. For the majority of the studies, the mitochondrial modulators were followed by a combined challenge of 100μM AITC & 1μM capsaicin to identify neurons that express either TRPA1 or TRPV1 channels. Sub-millimolar AITC is a selective agonist of TRPA1 [4,11,32]; capsaicin is a selective agonist of TRPV1 [3,11,33]. Lastly, cells were challenged with 75mM KCl to facilitate identification of neurons and 5μM ionomycin (calcium positive control). In one set of experiments, neurons from TRPV1^{-/-} mice were exposed to antimycin A (10μM), followed by H₂O₂ (300μM) and AITC (100μM), prior to KCl (75mM) and ionomycin (5μM). In another set of experiments, neurons were perfused with 10mM HEPES buffer with a calculated [Ca²⁺]_{free} of 75nM (154mM NaCl, 1mM KCl, 1.2mM MgCl₂, 0.71mM CaCl₂, 2mM EGTA, 5.6mM D-glucose) for 1 minute prior to, during, and for 2 minutes after exposure to mitochondrial modulators (antimycin A, 10μM; CCCP, 10μM; rotenone, 5μM) or vehicle (0.1% DMSO). Neurons were then perfused with normal 10mM HEPES (with 2.5mM CaCl₂) for 5 minutes prior to a combined challenge of 100μM AITC & 1μM capsaicin, then KCl (75mM) and ionomycin (5μM).

Images were taken every six seconds using microscopy (CoolSnap HQ2; Photometrics, Surrey, BC). Fura-2AM imaging (intracellular calcium concentration or [Ca²⁺]_i) was monitored by sequential excitation at 340 and 380nm (emission at 510nm) followed in most studies by either excitation at 470nm (emission at 525nm and 610nm) for mitochondrial polarization (JC-1), or 535nm (emission at 610nm) for superoxide production (MitoSOX).

2.4 Imaging analysis

Images were analyzed using Nikon Elements (Nikon, Melville, NY). Each individual neuron was analyzed separately using a region of interest (ROI) that encompassed the entire intracellular region. If required, ROIs were tracked over time to account for any cellular movement. For each imaging method (Fura-2AM, MitoSOX, and JC-1), ROIs with an unstable baseline, noisy baseline or insufficient loading were eliminated from the analysis. For Fura-2AM imaging, cells which failed to exhibit an increase in $[Ca^{2+}]_i$ to both AITC & capsaicin and KCl challenges ($> 30\%$ the ionomycin maximal response) were eliminated. Additionally, neurons that possessed an initial JC-1 red/green (525nm/610nm) ratio under 0.5 were eliminated as this indicated mitochondrial depolarization prior to the start of the experiment. For statistical analyses, we analyzed the maximal Fura-2AM, JC-1 and MitoSOX responses during the three-minute drug treatment (see below for calculations).

Relative changes in $[Ca^{2+}]_i$ were determined ratiometrically (R) using Fura-2 fluorescence: 340nm/380nm. As such the impact of variations in Fura-2AM loading are negated. The average calcium response to the combined AITC and capsaicin was used to classify A1/V1+ vs. A1-V1- neurons: A1/V1+ neurons had an $R_{AITC/Caps} > (R_{bl} + 2 * SD_{bl})$, where $R_{AITC/Caps}$ is the average 340/380 ratio during AITC/capsaicin treatment, R_{bl} is the baseline 340/380 ratio prior to treatment, and SD_{bl} is the standard deviation of R_{bl} . In the time series analyses, responses are presented as the change of the 340/380 ratio ($\Delta R = R_1 - R_0$). In the bar graphs, scatterplots and statistical analyses, the response to mitochondrial modulation was determined using the maximal $\Delta 340/380$ ($\Delta R_{max} = R_{max} - R_0$) for each neuron. An A1/V1+ neuron was defined as 'responding' to a particular mitochondrial agent if the $[Ca^{2+}]_i$ ΔR_{max} was greater than $3 * SD$ of the ΔR_{max} of A1-V1- neurons: $\Delta R_{max(A1/V1+)} > \Delta R_{max(A1-V1-)} + 3 * SD_{(A1-V1-)}$ where $\Delta R_{max(A1/V1+)}$ is the maximal response to mitochondrial modulation in an individual A1/V1+ neuron, $\Delta R_{max(A1-V1-)}$ is the average maximal response in A1-V1- neurons, and $SD_{(A1-V1-)}$ is the standard deviation of $\Delta R_{max(A1-V1-)}$. We have evaluated the effect of Fura-2AM loading on the calcium responses to mitochondrial modulation in these experiments and determined that there is no correlation between Fura-2 intensity at 380nm at baseline, an indicator of Fura-2AM loading, and the magnitude of ΔR_{max} (data not shown). This suggests that the effects of calcium buffering by Fura-2 are negligible in the dissociated vagal neurons used in these studies.

Mitochondrial superoxide production was analyzed using MitoSOX fluorescence (F, excitation at 535nm). Given that the reaction of superoxide with MitoSOX red is irreversible and that baseline physiologic ROS production by mitochondria will vary between individual neurons, we have chosen to correct for the slope in the time series studies using $F_{1(adjusted)} = F_1 - (S_0 * t)$, where F_1 is the raw fluorescence at a given timepoint (in arbitrary fluorescent units), S_0 is the slope of the baseline (arbitrary fluorescent units/s) and t is time of the F_1 measurement (in seconds). As MitoSOX loading varies between individual neurons, we have normalized the slope corrected data: $F_{1(adjusted)}/F_{0(adjusted)}$, where $F_{1(adjusted)}$ is the slope corrected fluorescence at a given timepoint and $F_{0(adjusted)}$ is the average of the slope corrected baseline. In order to determine the percentage of neurons that exhibited meaningful mitochondrial superoxide production compared to vehicle, we calculated the percentage of neurons whose individual maximal $F_{1(adjusted)}/F_{0(adjusted)}$ was greater than the average maximal $F_{1(adjusted)}/F_{0(adjusted)}$ for vehicle treatment + $3 * standard deviation$ of the maximal $F_{1(adjusted)}/F_{0(adjusted)}$ for vehicle treatment.

Mitochondrial polarization was determined using JC-1 fluorescence at both the green (525nm, which measures the monomeric form of JC-1) and red (610nm, which measures the aggregated form of JC-1) emission wavelengths. JC-1 accumulates in negatively charged mitochondria and forms 'red' aggregates. Upon mitochondrial depolarization, JC-1 disperses into

the cytosol as the 'green' monomeric form. As mentioned above, the 525nm/610nm ratio was used to identify neurons with depolarized mitochondria at baseline. However, we chose to determine the effect of mitochondrial modulation on mitochondrial polarization using only the 'green' monomeric form (F, 525nm fluorescence), as JC-1 fluorescence of 'red' aggregates is susceptible to quenching, prone to oxidation and requires ~90 minutes to reach equilibrium (versus ~15 minutes for monomers) [34]. Data were normalized (F_1/F_0) where F_1 is the emission fluorescence at 610nm at a given time point and F_0 is the baseline emission fluorescence at 610nm. This normalization process allowed for the calculation of the relative change of mitochondrial membrane potential independent of baseline polarization and JC-1 loading. In order to determine the percentage of neurons that exhibited meaningful mitochondrial depolarization compared to vehicle, we calculated the percentage of neurons whose individual maximal F_1/F_0 was greater than the average maximal F_1/F_0 for vehicle treatment + 3 * standard deviation of the maximal F_1/F_0 for vehicle treatment.

2.5 Statistical analyses

Statistical analyses were performed using R studio using maximal responses of the normalized responses observed during the three-minute drug treatment. To determine statistical differences in calcium response, mitochondrial polarization, and ROS production between mitochondrial agents and specific neuronal populations we performed two-way ANOVAs followed by post hoc comparison using the Bonferroni correction. To evaluate the correlation between cytosolic calcium and ROS production/mitochondrial depolarization, we performed a one-tailed Pearson correlation. A chi square test for homogeneity was used to evaluate the percentage of responding neurons for each inhibitor. A p value of 0.05 was taken as the threshold for significance.

2.6 Chemicals

Fura-2AM was purchased from TEFLabs (Austin, TX). MitoSOX Red, JC-1, and DMSO were purchased from Thermo Fisher Scientific (Waltham, MA). Ionomycin was purchased from LKT Laboratories (St. Paul, MN). All other reagents were purchased from Sigma-Aldrich (St. Louis, MO).

3. Results

3.1 Correlation between mitochondrial superoxide production and cytosolic calcium responses

Endogenous mediators modulate mitochondria at several different sites, thus we investigated neuronal responses to three mitochondrial agents: antimycin A (Complex III inhibitor), CCCP (uncoupling agent) and rotenone (Complex I inhibitor). We evaluated the contribution of mitochondrial superoxide production to neuronal activation by simultaneously measuring mitochondrial superoxide (MitoSOX Red) and cytosolic calcium (Fura-2AM) in dissociated vagal neurons using live cell co-imaging in response to antimycin A (10 μ M, n = 282 from 8 experiments), CCCP (10 μ M, n = 266 from 10 experiments), rotenone (5 μ M, n = 177 from 6 experiments) or DMSO vehicle (0.1%, n = 122 from 7 experiments). Approximately 60% of vagal sensory neurons were defined as A1/V1+, i.e. they subsequently responded to a combined treatment of 1 μ M capsaicin and 100 μ M AITC. All three agents produced a substantially larger increase in $[Ca^{2+}]_i$ in the A1/V1+ neuronal population compared to the A1-V1- population ($p < 0.05$) (Fig 1A, 1B, 1C and 1I). Indeed the vehicle also produced a minor, yet significant, increase in $[Ca^{2+}]_i$ in A1/V1+ neurons versus A1-V1- neurons ($p < 0.05$) (Fig 1D and 1I).

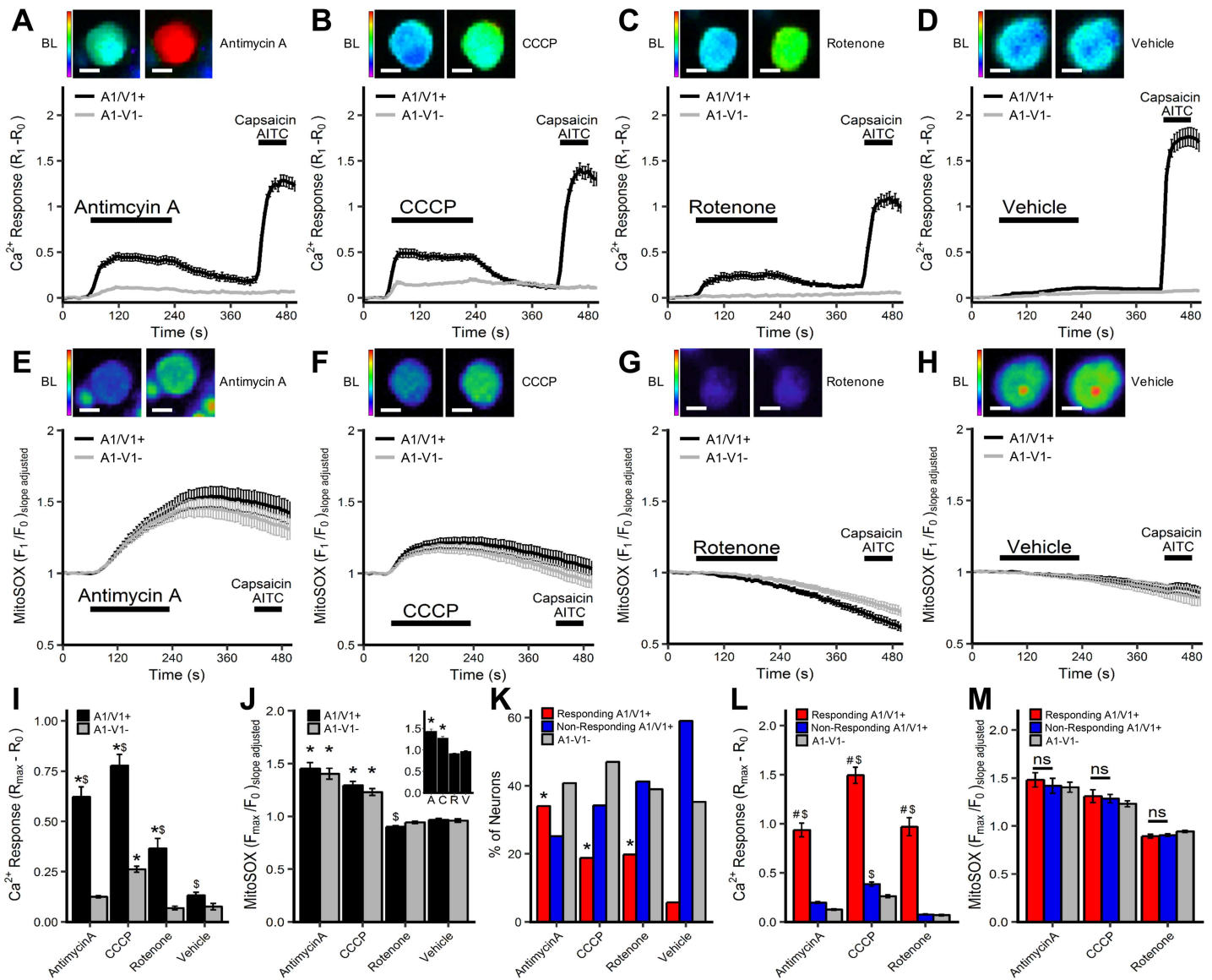


Fig 1. [Ca²⁺]_i and mitochondrial superoxide responses of vagal neurons to antimycin A, CCCP, rotenone and vehicle. Mean \pm SEM [Ca²⁺]_i responses (A–D) and mitochondrial superoxide (MitoSOX) responses (E–H) in A1/V1+ (black line) and A1-V1- (grey line) neurons treated with 10 μ M antimycin A (A, E), 10 μ M CCCP (B, F), 5 μ M rotenone (C, G) and 0.1% DMSO (D, H). Each panel includes representative Fura-2AM/MitoSOX image of a A1/V1+ neuron before and after treatment with the mitochondrial agent. A1/V1+ neurons are defined by increase in [Ca²⁺]_i following AITC/Caps treatment. (I) Mean \pm SEM maximal [Ca²⁺]_i response of A1/V1+ and A1-V1- neurons. (J) Mean \pm SEM maximal mitochondrial superoxide response of A1/V1+ and A1-V1- neurons (insert, mean \pm SEM maximal mitochondrial superoxide response of all neurons). (K) Percentage of neurons defined as ‘responding’ A1/V1+ neurons, ‘non-responding’ A1/V1+ neurons and A1-V1- neurons. (L) Mean \pm SEM maximal [Ca²⁺]_i response of ‘responding’ A1/V1+ neurons, ‘non-responding’ A1/V1+ neurons and A1-V1- neurons. (M) Mean \pm SEM maximal mitochondrial superoxide response of ‘responding’ A1/V1+ neurons, ‘non-responding’ A1/V1+ neurons and A1-V1- neurons. * denotes significant difference compared to vehicle ($p < 0.05$), \$ denotes significant difference between A1/V1+ and A1-V1- groups ($p < 0.05$), # denotes significant difference between ‘responding’ and ‘non-responding’ A1/V1+ groups ($p < 0.05$), ns denotes non-significance ($p > 0.05$).

<https://doi.org/10.1371/journal.pone.0197106.g001>

Nevertheless the increase in [Ca²⁺]_i in A1/V1+ neurons in response to antimycin A, CCCP and rotenone was significantly greater than that evoked by vehicle ($p < 0.05$) (Fig 1I). This data is consistent with our previous studies demonstrating antimycin A evoked calcium transients that were dependent on extracellular calcium and TRPA1 and TRPV1 [28]. Only CCCP evoked an increase in [Ca²⁺]_i in A1-V1- neurons that was greater than vehicle ($p < 0.05$) (Fig 1B, 1D and 1I).

MitoSOX measurements in the dual imaging studies showed that antimycin A and CCCP evoked significant mitochondrial superoxide production compared to vehicle in A1/V1+ neurons, A1-V1- neurons and the total neuronal population ($p < 0.05$) (Fig 1E, 1F, 1H and 1J) ($p < 0.05$). Despite the differences in calcium responses between A1/V1+ and A1-V1- populations, there was no differences in the magnitude of mitochondrial superoxide production in A1/V1+ and A1-V1- neurons evoked by either antimycin A or CCCP ($p > 0.05$) (Fig 1E, 1F and 1J). Rotenone failed to evoke significant mitochondrial superoxide production in either A1/V1+, A1-V1- or total populations compared to vehicle (Fig 1G, 1H and 1J). In general, rotenone had a minor inhibitory effect on the accumulation of MitoSOX fluorescence, which was more pronounced in the A1/V1+ population compared to the A1-V1- population ($p < 0.05$) (Fig 1G and 1J).

When we evaluated the calcium responses on a cell-by-cell basis we found that the mitochondrial agents only increased $[Ca^{2+}]_i$ beyond that evoked in A1-V1- neurons in a proportion of A1/V1+ neurons (see methods for definition of the threshold): antimycin A: 96/167, CCCP: 50/141, rotenone: 35/108 (Fig 1K). This 'responding' A1/V1+ population represents the A1/V1+ neurons 'activated' by the mitochondrial modulators and, consistent with this, the increase in $[Ca^{2+}]_i$ evoked by antimycin A, CCCP and rotenone was significantly greater in the 'responding' A1/V1+ population than either the 'non-responding' A1/V1+ or A1-V1- populations ($p < 0.05$) (Fig 1L). CCCP-evoked increases in $[Ca^{2+}]_i$ were marginally yet significantly greater in 'non-responding' A1/V1+ compared to A1-V1- neurons ($p < 0.05$), but this was not the case for either antimycin A or rotenone ($p > 0.05$) (Fig 1L). Importantly, there was no difference in mitochondrial superoxide production between 'responding' and 'non-responding' A1/V1+ neurons or A1-V1- neurons for any of the mitochondrial modulators ($p > 0.05$) (Fig 1M).

Scatterplot analysis of the calcium and MitoSOX responses (Fig 2) showed that mitochondrial superoxide production in response to antimycin A and CCCP was highly variable in all neuronal populations (i.e. 'responding' A1/V1+, 'non-responding' A1/V1+, and A1-V1- groups). Overall, only 40% and 23% of neurons exhibited an increase in mitochondrial superoxide production following treatment with antimycin A and CCCP, respectively (compared to 1.6% for vehicle, see methods for calculation). Antimycin A-evoked calcium responses correlated with mitochondrial superoxide production in the responding A1/V1+ population and in the total A1/V1+ population ($p < 0.05$) (Fig 2A, Table 1). However, there was no correlation between calcium and MitoSOX responses for CCCP in any neuronal population ($p > 0.05$) (Fig 2B, Table 1). Rotenone failed to evoke mitochondrial superoxide production in any neuronal population (0%) and as such there was no correlation between calcium and MitoSOX responses ($p > 0.05$) (Fig 2C, Table 1).

We have shown previously that antimycin A-induced calcium responses in nociceptive neurons were largely dependent on calcium influx through the cation channels TRPA1 and TRPV1 [28]. Here, we found in a separate series of Fura-2AM studies in vagal neurons ($n = 381$) that increases in $[Ca^{2+}]_i$ in A1/V1+ neurons in response mitochondrial modulation were largely dependent on extracellular calcium (Fig 3). There were no differences in calcium responses in A1/V1+ and A1-V1- neurons in response to antimycin A (10 μ M), CCCP (10 μ M), rotenone (5 μ M) or DMSO vehicle (0.1%) when extracellular calcium was buffered to 75 nM with EGTA ($p > 0.05$). Only CCCP evoked significantly greater responses in vagal neurons compared to vehicle ($p < 0.05$), suggesting that some of the CCCP-evoked calcium transient (in both A1/V1+ and A1-V1- neurons) was dependent on intracellular stores.

TRPA1 is directly activated by ROS [14–16], whereas there is little evidence that TRPV1 is activated by ROS [14,16,35]. We therefore investigated antimycin A-evoked Fura-2AM calcium and MitoSOX responses in vagal neurons from TRPA1^{-/-} and TRPV1^{-/-} mice ($n = 258$ from 9 experiments and $n = 201$ from 10 experiments, respectively). $[Ca^{2+}]_i$ and mitochondrial

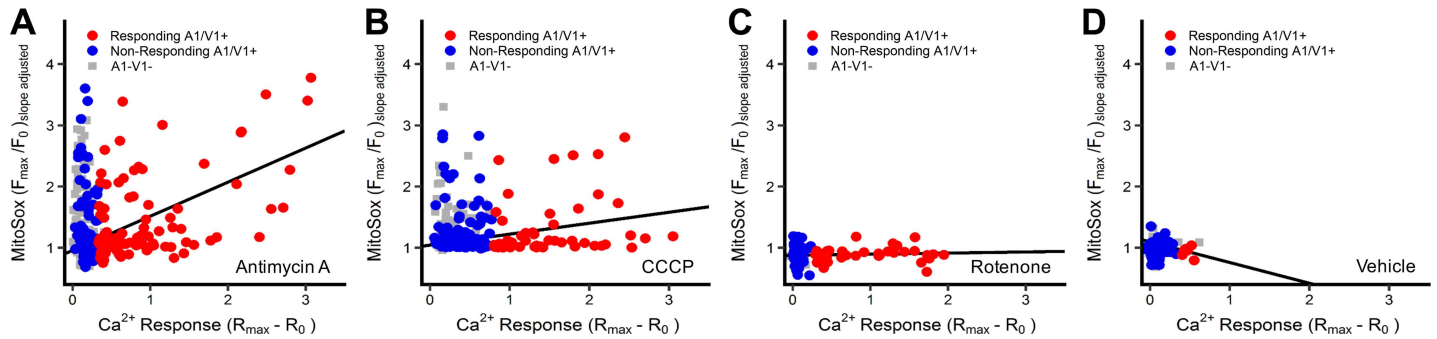


Fig 2. Mitochondrial superoxide responses correlates with $[Ca^{2+}]_i$ responses for antimycin A, but not CCCP or rotenone. Co-imaging of $[Ca^{2+}]_i$ and superoxide in neurons treated with 10 μ M antimycin A (A), 10 μ M CCCP (B), 5 μ M rotenone (C) and 0.1% DMSO (D). Trendlines depict the correlation in ‘responding’ A1/V1+ neurons. Slope and significance of each trendline is presented in Table 1.

<https://doi.org/10.1371/journal.pone.0197106.g002>

superoxide production correlated in ‘responding’ *trpv1*^{-/-} A1+ neurons ($p < 0.05$) (Fig 4A, Table 1) but not in ‘responding’ *trpa1*^{-/-} V1+ neurons ($p > 0.05$) (Fig 4B, Table 1). Similar to the wild-type A1/V1+ neurons, mitochondrial modulation with antimycin A failed to evoke calcium responses in all *trpv1*^{-/-} A1+ neurons, suggesting the possibility that some neurons expressing the TRPA1 channel were insensitive to ROS. Sequential exposure of vagal neurons from TRPV1^{-/-} mice ($n = 202$ from 7 experiments) to antimycin A (10 μ M), H₂O₂ (300 μ M) and then AITC (100 μ M), showed that a significant proportion of antimycin-insensitive, A1+ neurons did indeed respond to the H₂O₂ with an increase in calcium (Fig 4C and 4D). This data confirms the sensitivity of TRPA1 channels in these neurons to exogenously applied ROS H₂O₂.

3.2 Correlation between mitochondrial depolarization and cytosolic calcium responses

Given that our data suggests that mitochondrial superoxide is not the only determinant of mitochondrial modulation-induced A1/V1+ neuronal activation, we next investigated mitochondrial depolarization—another hallmark of mitochondrial dysfunction. We performed live cell co-imaging of cytosolic calcium (Fura-2AM) and mitochondrial polarization (JC-1) during treatment with antimycin A (10 μ M, $n = 90$ from 6 experiments), CCCP (10 μ M, $n = 210$

Table 1. Trendlines for the correlation of $[Ca^{2+}]_i$ and mitochondrial superoxide in subsets of vagal A1/V1+ neurons after treatment with antimycin A, CCCP and rotenone.

| | Responding A1/V1+ neurons | | | Non-Responding A1/V1+ neurons | | | All A1/V1+ neurons | | |
|----------------------------|---------------------------|----------|------|-------------------------------|------|------|--------------------|----------|------|
| | Slope | p | Sig. | Slope | p | Sig. | Slope | p | Sig. |
| Wild-type | | | | | | | | | |
| Antimycin A | 0.48 | 3.03E-08 | * | -0.04 | 0.99 | | 0.31 | 2.68E-06 | * |
| CCCP | 0.27 | 0.06 | | -0.03 | 0.72 | | 0.13 | 0.15 | |
| Rotenone | 0.41 | 0.31 | | -0.02 | 0.71 | | -0.06 | 0.55 | |
| Vehicle | -0.15 | 0.69 | | 0.10 | 0.13 | | 0.00 | 0.51 | |
| TRPV1^{-/-} | | | | | | | | | |
| Antimycin A | 0.04 | 0.23 | | -0.01 | 0.84 | | 0.05 | 0.10 | |
| TRPA1^{-/-} | | | | | | | | | |
| Antimycin A | 0.42 | 0.03 | * | -0.01 | 0.95 | | -0.04 | -0.07 | |

*: Denotes $p < 0.05$

<https://doi.org/10.1371/journal.pone.0197106.t001>

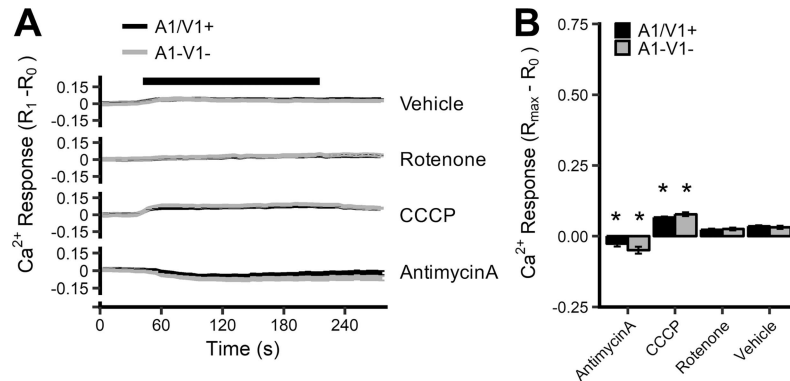


Fig 3. $[Ca^{2+}]_i$ responses of vagal neurons to antimycin A, CCCP, rotenone and vehicle in the nominal absence of extracellular calcium. (A) Mean \pm SEM $[Ca^{2+}]_i$ responses in A1/V1+ (black line) and A1-V1- (grey line) neurons treated with 10 μ M antimycin A, 10 μ M CCCP, 5 μ M rotenone and 0.1% DMSO. Blocked line denotes stimulus application. A1/V1+ neurons are defined by increase in $[Ca^{2+}]_i$ following AITC/Caps treatment in the presence of 2.5mM $CaCl_2$ (data not shown). (B) Mean \pm SEM maximal $[Ca^{2+}]_i$ response of A1/V1+ and A1-V1- neurons. * denotes significant difference compared to vehicle ($p < 0.05$), \$ denotes significant difference between A1/V1+ and A1-V1- groups ($p < 0.05$).

<https://doi.org/10.1371/journal.pone.0197106.g003>

from 10 experiments), rotenone (5 μ M, n = 112 from 7 experiments) and DMSO vehicle (0.1%, n = 129 from 8 experiments).

Again, approximately 60% of vagal sensory neurons were defined as A1/V1+, and all three mitochondrial agents evoked substantially larger increases in $[Ca^{2+}]_i$ in the A1/V1+ neuronal population compared to the A1-V1- population ($p < 0.05$) (Fig 5A, 5B, 5C and 5I), and these responses were significantly greater than those evoked by vehicle ($p < 0.05$) (Fig 5D and 5I). Again, CCCP alone evoked an increase in $[Ca^{2+}]_i$ in A1-V1- neurons that was greater than vehicle ($p < 0.05$) (Fig 5B, 5D and 5I). Antimycin A and CCCP both caused significant mitochondrial depolarization compared to vehicle ($p < 0.05$) but there were no differences between A1/V1+ and A1-V1- populations ($p > 0.05$) (Fig 5E, 5F, 5H and 5I). Mitochondrial depolarization occurred in 97% and 80% of neurons in response to antimycin A and CCCP, respectively (compared to 0.8% for vehicle). Although rotenone failed to evoke significant mitochondrial depolarization compared to vehicle in the total, A1/V1+ and A1-V1- populations overall (Fig

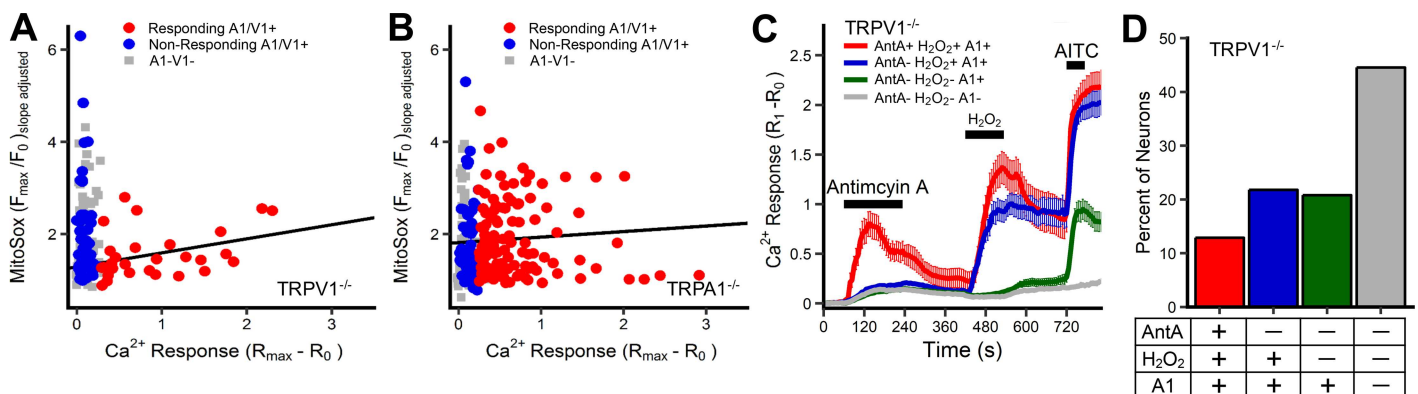


Fig 4. Antimycin A-induced $[Ca^{2+}]_i$ responses correlates with mitochondrial superoxide responses in *trpv1*^{-/-} A1+ neurons but not *trpa1*^{-/-} V1+ neurons. Co-imaging of $[Ca^{2+}]_i$ and superoxide in neurons treated with 10 μ M antimycin A in neurons from TRPV1^{-/-} (A) and TRPA1^{-/-} (B) mice. Trendlines depict the correlation in 'responding' neurons. Slope and significance of each trendline is presented in Table 1. (C) Mean \pm SEM $[Ca^{2+}]_i$ responses in neurons from TRPV1^{-/-} mice treated with 10 μ M antimycin A, 300 μ M H₂O₂ and 100 μ M AITC. Neurons allocated to groups based upon sensitivity to the stimuli. A1+ defined by response to AITC. (D) Percentage of neurons from TRPV1^{-/-} mice allocated to groups shown in C.

<https://doi.org/10.1371/journal.pone.0197106.g004>

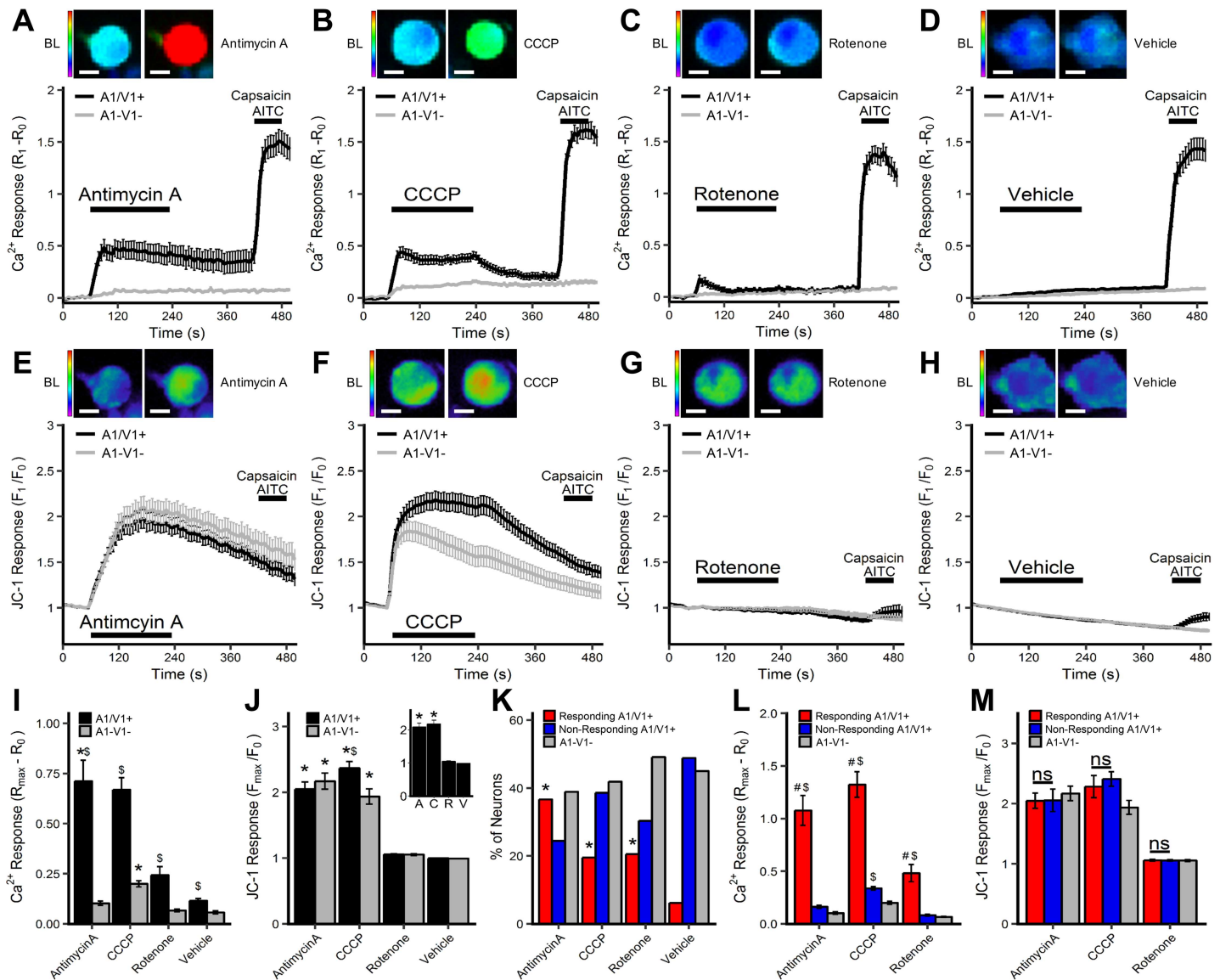


Fig 5. $[Ca^{2+}]_i$ and mitochondrial polarization responses of vagal neurons to antimycin A, CCCP, rotenone and vehicle. Mean \pm SEM $[Ca^{2+}]_i$ responses (A–D) and mitochondrial polarization (JC-1) responses (E–H) in A1/V1+ (black line) and A1-V1- (grey line) neurons treated with 10 μ M antimycin A (A, E), 10 μ M CCCP (B, F), 5 μ M rotenone (C, G) and 0.1% DMSO (D, H). Each panel includes representative Fura-2AM/JC-1 image of an A1/V1+ neuron before and after treatment with the mitochondrial agent. A1/V1+ neurons are defined by increase in $[Ca^{2+}]_i$ following AITC/Caps treatment. (I) Mean \pm SEM maximal $[Ca^{2+}]_i$ response of A1/V1+ and A1-V1- neurons. (J) Mean \pm SEM maximal mitochondrial depolarization of A1/V1+ and A1-V1- neurons (insert, mean \pm SEM maximal mitochondrial depolarization of all neurons). (K) Percentage of neurons defined as ‘responding’ A1/V1+, ‘non-responding’ A1/V1+ and A1-V1-. (L) Mean \pm SEM maximal $[Ca^{2+}]_i$ response of ‘responding’ A1/V1+, ‘non-responding’ A1/V1+ and A1-V1-. (M) Mean \pm SEM maximal mitochondrial depolarization of ‘responding’ A1/V1+, ‘non-responding’ A1/V1+ and A1-V1-. * denotes significant difference compared to vehicle ($p < 0.05$), \$ denotes significant difference between A1/V1+ and A1-V1- groups ($p < 0.05$), # denotes significant difference between ‘responding’ and ‘non-responding’ A1/V1+ groups ($p < 0.05$), ns denotes non-significance ($p > 0.05$).

<https://doi.org/10.1371/journal.pone.0197106.g005>

5G and 5J), rotenone did evoke mitochondrial depolarization in 38% of neurons (compared to 0.8% for vehicle).

Analysis of individual neuronal responses showed again that the mitochondrial agents only increased $[Ca^{2+}]_i$ beyond that evoked in A1-V1- neurons in a proportion of A1/V1+ neurons: antimycin A: 33/55, CCCP: 41/122, rotenone: 23/57 (Fig 5K). Indeed, the increase in $[Ca^{2+}]_i$ evoked by antimycin A, CCCP and rotenone was significantly greater in the ‘responding’ A1/

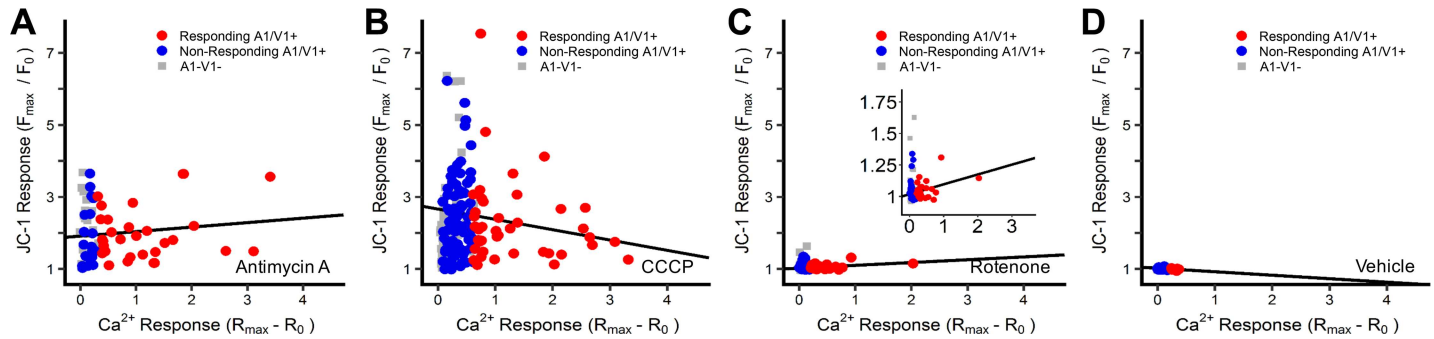


Fig 6. Mitochondrial depolarization responses correlates with $[Ca^{2+}]_i$ responses for rotenone, but not antimycin A or CCCP. Co-imaging of $[Ca^{2+}]_i$ and mitochondrial polarization in neurons treated with 10 μ M antimycin A (A), 10 μ M CCCP (B), 5 μ M rotenone (C) and 0.1% DMSO (D). Trendlines depict the correlation in ‘responding’ A1/V1+ neurons. Slope and significance of each trendline is presented in Table 2.

<https://doi.org/10.1371/journal.pone.0197106.g006>

V1+ population than either the ‘non-responding’ A1/V1+ or A1-V1- populations ($p < 0.05$) (Fig 5L). Notably, there were no differences in mitochondrial depolarization between ‘responding’ A1/V1+ and ‘non-responding’ A1/V1+ neurons for each of the agents ($p > 0.05$) (Fig 5M). Using scatterplots of the cell-by-cell responses, we found there was no correlation of calcium responses evoked by either antimycin A or CCCP to mitochondrial depolarization in ‘responding’ A1/V1+ neurons ($p > 0.05$) (Fig 6A and 6B, Table 2). Nevertheless, there was a minor, yet significant correlation of rotenone-induced calcium responses to mitochondrial depolarization in ‘responding’ A1/V1+ neurons ($p > 0.05$) (Fig 6C, Table 2), consistent with the finding that some neurons exhibited mitochondrial depolarization with rotenone.

4. Discussion

Nociceptive activation is a hallmark of inflammation in multiple organs, resulting in debilitating symptoms (e.g. pain) and reflexes (e.g. vasodilation, edema, bronchospasm, etc.) [36–38]. While inflammatory signaling pathways involving TNF α , ceramides and neurotrophins inhibit complexes of the mETC and induce mitochondrial dysfunction (ROS production, depolarization, and calcium release) [24–27], the mechanisms linking these factors to C-fiber activity are largely unknown. In a previous study, we demonstrated that inhibition of mETC complex III with antimycin A activated bronchopulmonary C-fibers via the activation of TRPA1 and TRPV1 [28]– Ca^{2+} -permeable cation channels selectively expressed on many nociceptive sensory neurons [7,28,39]. However, the influence of specific aspects of mitochondrial function on TRPA1 and TRPV1 activation remains unknown. Here, we investigated the correlation of

Table 2. Trendlines for the correlation of $[Ca^{2+}]_i$ and mitochondrial depolarization in subsets of vagal A1/V1+ neurons after treatment with antimycin A, CCCP and rotenone.

| | Responding A1/V1+ neurons | | | Non-Responding A1/V1+ neurons | | | All A1/V1+ neurons | | |
|------------------|---------------------------|------|------|-------------------------------|------|------|--------------------|------|------|
| | Slope | p | Sig. | Slope | p | Sig. | Slope | p | Sig. |
| Wild-type | | | | | | | | | |
| Antimycin A | 0.15 | 0.22 | | 0.02 | 0.13 | | 0.09 | 0.26 | |
| CCCP | -0.12 | 0.88 | | 0.03 | 0.03 | * | -0.05 | 0.82 | |
| Rotenone | 2.08 | 0.03 | * | -0.12 | 0.87 | | 0.71 | 0.09 | |
| Vehicle | -0.45 | 0.69 | | 0.13 | 0.37 | | -0.48 | 0.81 | |

*: Denotes $p < 0.05$

<https://doi.org/10.1371/journal.pone.0197106.t002>

mitochondrial depolarization and superoxide production on calcium fluxes in dissociated vagal neurons following mitochondrial modulation.

As inflammatory signaling inhibits the mETC at multiple sites, we performed these experiments using three mitochondrial agents: antimycin A (complex III inhibitor), rotenone (complex I inhibitor), and CCCP (mitochondrial uncoupling agent). Here, we found that all three agents caused robust increases in $[Ca^{2+}]_i$ in the vagal A1/V1+ neuronal population. These data are consistent with our previous study that antimycin A evoked a selective increase in $[Ca^{2+}]_i$ in A1/V1+ vagal neurons that was abolished by the removal of extracellular Ca^{2+} or by the genetic and pharmacological blockade of the nociceptive-specific ion channels TRPA1 and TRPV1 [28]. Given that TRPA1/TRPV1 were required for antimycin A-induced bronchopulmonary C-fiber activation [28], it is likely that the mitochondrial agent-evoked increases in $[Ca^{2+}]_i$ in A1/V1+ neurons observed in this study represents preferential activation of A1/V1+ neurons. However, not all A1/V1+ neurons 'responded' to mitochondrial modulation: approximately 60%, 35% and 35% of A1/V1+ neurons exhibited an increase in $[Ca^{2+}]_i$ to antimycin A, CCCP and rotenone, respectively. In general, antimycin A and CCCP evoked greater increases in $[Ca^{2+}]_i$ in 'responding' A1/V1+ neurons than rotenone. There was no correlation between responses in individual A1/V1+ neurons and their proximity to other neurons (data not shown), suggesting that calcium responses in each neuron was independent of the effects of mitochondrial modulation in other neurons.

Mitochondrial modulation can evoke ROS production, most notably at complexes I and III, when electrons leak and incompletely oxidize O_2 resulting in $O_2^{\cdot-}$ (superoxide) formation [40–43]. Superoxide is membrane impermeable and highly reactive, thus is capable of damaging DNA, proteins and lipids. In cells, superoxide dismutase rapidly converts superoxide to H_2O_2 which is membrane permeable but less reactive [44]. Here, we found that antimycin A increased mitochondrial superoxide production acutely in both A1/V1+ and A1-V1- neurons. Furthermore, there was no difference in the mitochondrial superoxide production evoked by antimycin A between the 'responding' A1/V1+ and 'non-responding' neurons. Nevertheless, there was a significant correlation between antimycin A-evoked mitochondrial superoxide production and the magnitude of calcium responses in 'responding' A1/V1+ neurons. Our interpretation of these data is that mitochondrial superoxide produced by antimycin A can lead to A1/V1+ neuronal activation, but this is dependent on another unknown factor that is not present in all A1/V1+ neurons. It should be noted that only 40% of all neurons exhibited increased superoxide production in response to antimycin A, raising the possibility that some neurons are insensitive to this mitochondrial modulating agent. However, this seems unlikely given the observation that 97% of neurons exhibited antimycin A-induced mitochondrial depolarization.

Both superoxide and H_2O_2 are potent activators of TRPA1 [15,16]. Here, we found a significant correlation between antimycin A-evoked mitochondrial superoxide production and the magnitude of calcium responses in 'responding' $trpv1^{-/-}$ A1+ neurons, whose responses are presumed to be mediated by ROS-sensitive TRPA1 alone [28]. Nevertheless, some $trpv1^{-/-}$ A1+ neurons failed to be activated despite substantial superoxide production, thus again suggesting that some other unknown factor is required for mitochondrial ROS-mediated TRPA1 activation. Separate studies confirmed that many non-responding $trpv1^{-/-}$ A1+ neurons were activated by exogenously-applied H_2O_2 . Importantly, there was no correlation between antimycin A-evoked mitochondrial superoxide production and the magnitude of calcium responses in 'responding' $trpa1^{-/-}$ V1+ neurons, whose responses are likely mediated by TRPV1 [28]. There is little evidence to suggest that TRPV1 is a major target of ROS and oxidative stress: TRPV1 is not activated by physiological concentrations of H_2O_2 [16,35] or most electrophilic products of lipid peroxidation [45], although it is activated by high concentrations of

4-oxononenal [11]. Instead, TRPV1 is activated by PIP₂ hydrolysis, GPCR signaling and arachidonic acid metabolites [45–48]. Our data further suggests that TRPV1-mediated activation by antimycin A is not downstream of superoxide production.

Like antimycin A, CCCP evoked significant mitochondrial superoxide production in all neuronal populations, consistent with previous reports in isolated rat brain mitochondria [49], although other studies indicate that uncoupling agents such as CCCP do not increase ROS production [50,51]. However, there was no correlation between CCCP-induced mitochondrial superoxide production and the magnitude of calcium responses in ‘responding’ A1/V1+ neurons. Approximately 80% of neurons exhibited mitochondrial depolarization to CCCP, but there were no significant differences between the mitochondrial depolarization in ‘responding’ A1/V1+ and ‘non-responding’ neurons and there was no correlation between mitochondrial depolarization and the magnitude of calcium responses in ‘responding’ A1/V1+ neurons. We therefore conclude that factors other than mitochondrial superoxide production determine the CCCP-induced activation of A1/V1+ neurons and that mitochondrial depolarization alone is unable to account for these responses.

Rotenone failed to cause mitochondrial superoxide production in any neuronal population. Indeed, rotenone decreased baseline mitochondrial ROS production in A1/V1+ neurons. Previous studies have shown that rotenone can increase or decrease ROS production depending on metabolism of complex I versus complex II substrates [42,52]. Despite the lack of superoxide production, rotenone evoked an increase in [Ca²⁺]_i in approximately 35% of A1/V1+ neurons in this study. Although rotenone caused mitochondrial depolarization in approximately 38% of all vagal neurons, there were no significant differences between the mitochondrial depolarization in ‘responding’ A1/V1+ and ‘non-responding’ neurons. Nevertheless, there was a significant correlation between rotenone-evoked mitochondrial depolarization and the magnitude of calcium responses in ‘responding’ A1/V1+ neurons. This suggests that mitochondrial depolarization alone can lead to A1/V1+ neuronal activation, but again this is dependent on another unknown factor that is not present in all A1/V1+ neurons.

Our data indicates that mitochondrial modulators (in particular antimycin A and CCCP) evoke mitochondrial superoxide production in a limited percentage of neurons despite the evident mitochondrial depolarization in the majority of neurons. The present study used quantitative measurements of mitochondrial superoxide using MitoSOX, which is neither ratiometric nor reversible, making it possibly susceptible, despite our efforts to normalize the data, to variations in loading and baseline redox state. MitoSOX is targeted to the mitochondrial matrix, thus it is possible that some of the superoxide produced from complex I and III may evade MitoSOX detection following its release into the intermembrane space [41,53,54]. ROS produced within sensory neurons has 3 potential fates: reacting with signaling pathways, with endogenous antioxidant systems (e.g. glutathione) or with the ROS-sensitive dye. As such, the quantification of ROS production may be susceptible to significant error on a cell-by-cell basis. Nevertheless, even a qualitative analysis suggests that (A) mitochondrial modulation does not evoke significant calcium responses in all A1/V1+ neurons and (B) significant ROS production does not necessarily evoke calcium responses in A1/V1+ neurons. This suggests that factors in addition to superoxide determine the TRPA1- and TRPV1-mediated calcium responses in A1/V1+ neurons. The identity of these factors is presently unknown, but it is possible that these either involve the activity of antioxidant systems or the spatial/temporal arrangement of mitochondria, TRP channels and signaling molecules. Our rotenone studies suggest that mitochondrial depolarization is able to contribute, but experiments with CCCP (and antimycin A) indicate that mitochondrial depolarization is not guaranteed to result in significant calcium responses in A1/V1+ neurons. How mitochondrial depolarization could contribute to A1/V1+ neuronal activation is not yet known. Mitochondrial depolarization

causes calcium efflux from the matrix, and calcium is a regulator of multiple pathways such as phospholipases and protein kinases [55,56] that can alter TRP channel activity [45,57–59].

Unlike antimycin A and rotenone, CCCP evoked a significant increase in $[Ca^{2+}]_i$ in A1-V1- neurons, although these were much smaller than those in A1/V1+ neurons. As such, the threshold for determining the calcium ‘responsiveness’ of a particular neurons is greater for CCCP treatments. A1-V1- neurons do not express TRPA1 or TRPV1. Thus, the source of the CCCP-evoked calcium responses in A1-V1- is presently unknown. It is possible that calcium release from the mitochondrial matrix after robust mitochondrial depolarization contributes to these calcium transients [60], and this is consistent with (A) the significant calcium responses with CCCP in the nominal absence of extracellular calcium and (B) the significant correlation between CCCP-evoked mitochondrial depolarization and the magnitude of calcium responses in A1-V1- neurons (slope 0.035, $p < 0.05$, data not shown).

The present study has investigated the correlation between mitochondrial ROS/depolarization and calcium transients evoked by mitochondrial modulators in vagal neurons. Our previous study identified the critical role of TRPA1 and TRPV1 in antimycin A-induced calcium responses and bronchopulmonary C-fiber activation [28]. Although the specific role of TRPA1 and TRPV1 has not been extensively investigated in the present study, our data is consistent with TRPA1 and TRPV1 mediating the mitochondrial modulator-evoked calcium responses. It is important to note, however, that TRP channel sensitivity itself is not static and that multiple intracellular pathways, including oxidative stress, can promote either sensitization or desensitization of TRPA1 and TRPV1 channels [3,61–64]. Furthermore, TRPA1 and TRPV1 have been reported to functionally modulate each other’s sensitivity [65,66]. Although not addressed here, it is possible that mitochondrial modulation may impact TRP function beyond channel activation.

In summary, we have shown that mitochondrial modulation by antimycin A-induced TRPA1-mediated calcium responses in vagal A1/V1+ neurons correlates with mitochondrial superoxide production, but that other factors including mitochondrial depolarization may contribute to A1/V1+ neuronal calcium responses via TRPV1 and downstream of complex I inhibition and mitochondrial uncoupling. It should be emphasized that the conclusions here are based upon correlations, which do not necessarily imply causation. Thus, we note that these studies do not show a conclusive role of superoxide production in the A1/V1+ neuronal calcium responses by mitochondrial modulators. Furthermore, we have focused our present study on dissociated vagal neurons and it is possible that mechanisms linking mitochondrial superoxide production and depolarization with TRP channel activation may be different within sensory terminals in vivo. More studies are needed to fully understand the events linking mitochondrial dysfunction and nociceptor activation.

Supporting information

S1 Dataset. Raw data for dual imaging of Fura2 and mitoSOX.

(XLSX)

S2 Dataset. Raw data for dual imaging of Fura2 and JC-1.

(XLSX)

Author Contributions

Conceptualization: Thomas E. Taylor-Clark.

Data curation: Katherine R. Stanford.

Formal analysis: Katherine R. Stanford.

Funding acquisition: Thomas E. Taylor-Clark.

Investigation: Katherine R. Stanford.

Methodology: Katherine R. Stanford, Thomas E. Taylor-Clark.

Supervision: Thomas E. Taylor-Clark.

Visualization: Katherine R. Stanford, Thomas E. Taylor-Clark.

Writing – original draft: Katherine R. Stanford.

Writing – review & editing: Thomas E. Taylor-Clark.

References

1. Marchand F, Perretti M, McMahon SB. Role of the immune system in chronic pain. *Nat Neurosci*. 2005; 6(7):521–32.
2. McMahon SB, La Russa F, Bennett DLH. Crosstalk between the nociceptive and immune systems in host defence and disease. *Nat Rev Neurosci*. 2015; 16(7):389–402. <https://doi.org/10.1038/nrn3946> PMID: 26087680
3. Caterina MJ, Schumacher MA, Tominaga M, Rosen TA, Levine JD, Julius D. The capsaicin receptor: a heat-activated ion channel in the pain pathway. *Nature*. 1997; 389(6653):816–24. <https://doi.org/10.1038/39807> PMID: 9349813
4. Jordt S, Bautista DM, Chuang H, Meng ID, Julius D. Mustard oils and cannabinoids excite sensory nerve fibres through the TRP channel ANKTM1. *Nature*. 2004; 427(1):260–5.
5. Kobayashi K, Fukuoka T, Obata K, Yamanaka H, Dai Y, Tokunaga A, et al. Distinct expression of TRPM8, TRPA1, and TRPV1 mRNAs in rat primary afferent neurons with A δ /C-fibers and colocalization with Trk receptors. *J Comp Neurol*. 2005; 493(4):596–606. <https://doi.org/10.1002/cne.20794> PMID: 16304633
6. Michael GJ, Priestley JV. Differential expression of the mRNA for the vanilloid receptor subtype 1 in cells of the adult rat dorsal root and nodose ganglia and its downregulation by axotomy. *J Neurosci*. 1999; 19(5):1844–54. PMID: 10024368
7. Nassenstein C, Kwong K, Taylor-Clark TE, Kollarik M, Macglashan DM, Braun A, et al. Expression and function of the ion channel TRPA1 in vagal afferent nerves innervating mouse lungs. *J Physiol*. 2008; 586(6):1595–604. <https://doi.org/10.1113/jphysiol.2007.148379> PMID: 18218683
8. Ricco MM, Kummer W, Biglari B, Myers AC, Udem BJ. Interganglionic segregation of distinct vagal afferent fibre phenotypes in guinea-pig airways. *J Physiol*. 1996; 496(2):521–30.
9. Kollarik M, Dinh QT, Fischer A, Udem BJ. Capsaicin-sensitive and -insensitive vagal bronchopulmonary C-fibres in the mouse. *J Physiol*. 2003; 551(3):869–79.
10. Usoskin D, Furlan A, Islam S, Abdo H, Lönnerberg P, Lou D, et al. Unbiased classification of sensory neuron types by large-scale single-cell RNA sequencing. *Nat Neurosci*. 2015; 18(1):145–53. <https://doi.org/10.1038/nn.3881> PMID: 25420068
11. Taylor-Clark TE, McAlexander MA, Nassenstein C, Sheardown SA, Wilson S, Thornton J, et al. Relative contributions of TRPA1 and TRPV1 channels in the activation of vagal bronchopulmonary C-fibres by the endogenous autacoid 4-oxononenal. *J Physiol*. 2008; 586(14):3447–59. <https://doi.org/10.1113/jphysiol.2008.153585> PMID: 18499726
12. Taylor-Clark TE, Ghatta S, Bettner W, Udem BJ. Nitrooleic acid, an endogenous product of nitrative stress, activates nociceptive sensory nerves via the direct activation of TRPA1. *Mol Pharmacol*. 2009; 75(4):820–9. <https://doi.org/10.1124/mol.108.054445> PMID: 19171673
13. Macpherson LJ, Dubin AE, Evans MJ, Marr F, Schultz PG, Cravatt BF, et al. Noxious compounds activate TRPA1 ion channels through covalent modification of cysteines. *Nature*. 2007; 445(7127):541–5. <https://doi.org/10.1038/nature05544> PMID: 17237762
14. Andersson DA, Gentry C, Moss S, Bevan S. Transient receptor potential A1 is a sensory receptor for multiple products of oxidative stress. *J Neurosci*. 2008; 28(10):2485–94. <https://doi.org/10.1523/JNEUROSCI.5369-07.2008> PMID: 18322093
15. Takahashi N, Mizuno Y, Kozai D, Yamamoto S, Kiyonaka S, Shibata T, et al. Molecular characterization of TRPA1 channel activation by cysteine-reactive inflammatory mediators. *Channels*. 2008; 2(4):287–9. PMID: 18769139

16. Sawada Y, Hosokawa H, Matsumura K, Kobayashi S. Activation of transient receptor potential ankyrin 1 by hydrogen peroxide. *Eur J Neurosci*. 2008; 27(5):1131–42. <https://doi.org/10.1111/j.1460-9568.2008.06093.x> PMID: 18364033
17. Lishko PV., Procko E, Jin X, Phelps CB, Gaudet R. The Ankyrin Repeats of TRPV1 Bind Multiple Ligands and Modulate Channel Sensitivity. *Neuron*. 2007; 54(6):905–18. <https://doi.org/10.1016/j.neuron.2007.05.027> PMID: 17582331
18. von Düring M, Andres KH. Structure and functional anatomy of visceroreceptors in the mammalian respiratory system. *Prog Brain Res*. 1988; 74:139–54. PMID: 3055045
19. Hung KS, Hertweck MS, Hardy JD, Loosli CG. Ultrastructure of nerves and associated cells in bronchiolar epithelium of the mouse lung. *J Ultrastruct Res*. 1973; 43(5):426–37. PMID: 4578329
20. Mabalirajan U, Dinda AK, Kumar S, Roshan R, Gupta P, Sharma SK, et al. Mitochondrial structural changes and dysfunction are associated with experimental allergic asthma. *J Immunol*. 2008; 181(5):3540–8. PMID: 18714027
21. López-Armada MJ, Riveiro-Naveira RR, Vaamonde-García C, Valcárcel-Ares MN. Mitochondrial dysfunction and the inflammatory response. *Mitochondrion*. 2013; 13(2):106–18. <https://doi.org/10.1016/j.mito.2013.01.003> PMID: 23333405
22. Van Tilburg MAL, Zaki EA, Venkatesan T, Boles RG. Irritable Bowel Syndrome may be associated with maternal inheritance and mitochondrial DNA control region sequence variants. *Dig Dis Sci*. 2014; 59(7):1392–7. <https://doi.org/10.1007/s10620-014-3045-2> PMID: 24500451
23. Raby BA, Klanderma B, Murphy A, Mazza S, Camargo CA, Silverman EK, et al. A common mitochondrial haplogroup is associated with elevated total serum IgE levels. *J Allergy Clin Immunol*. 2007; 120(2):351–8. <https://doi.org/10.1016/j.jaci.2007.05.029> PMID: 17666217
24. Stadler J, Bentz BG, Harbrecht BG, Di Silvio M, Curran RD, Billiar T, et al. Tumor necrosis factor alpha inhibits hepatocyte mitochondrial respiration. *Ann Surg*. 1992; 216(5):539–46. PMID: 1444645
25. Zell R, Geck P, Werdan K, Boekstegers P. TNF- α and IL-1 α inhibit both pyruvate dehydrogenase activity and mitochondrial function in cardiomyocytes: Evidence for primary impairment of mitochondrial function. *Mol Cell Biochem*. 1997; 177(1–2):61–7. PMID: 9450646
26. Lopez-Armada M, Carame B, Marti M, Lires-Dean M, Fuentes-Boquete I, Arenas J, et al. Mitochondrial activity is modulated by TNF- α and IL-1 β in normal human chondrocyte cells. *Osteoarthritis Cartil*. 2006; 14(10):1011–22. <https://doi.org/10.1016/j.joca.2006.03.008> PMID: 16679036
27. Colell A, Morales A, Ferra C, García-Ruiz C, Colell A, Mari M, et al. Direct effect of ceramide on the mitochondrial electron transport chain leads to generation of reactive oxygen species. *J Biol Chem*. 1997; 272(17):11369–77. PMID: 9111045
28. Nesuashvili L, Hadley SH, Bahia PK, Taylor-Clark TE. Sensory nerve terminal mitochondrial dysfunction activates airway sensory nerves via transient receptor potential (TRP) Channels. *Mol Pharmacol*. 2013; 83(5):1007–19. <https://doi.org/10.1124/mol.112.084319> PMID: 23444014
29. Starkov AA, Fiskum G. Myxothiazol induces H₂O₂ production from mitochondrial respiratory chain. *Biochem Biophys Res Commun*. 2001; 281(3):645–50. <https://doi.org/10.1006/bbrc.2001.4409> PMID: 11237706
30. Chinopoulos C, Tretter L, Adam-Vizi V. Depolarization of in situ mitochondria due to hydrogen peroxide-induced oxidative stress in nerve terminals: inhibition of α -ketoglutarate dehydrogenase. *J Neurochem*. 1999; 73(1):220–8. PMID: 10386974
31. Li N, Oquendo E, Capaldi RA, Paul Robinson J, He YD, Hamadeh HK, et al. A systematic assessment of mitochondrial function identified novel signatures for drug-induced mitochondrial disruption in cells. *Toxicol Sci*. 2014; 142(1):261–73. <https://doi.org/10.1093/toxsci/ktu176> PMID: 25163676
32. Bautista DM, Jordt SE, Nikai T, Tsuruda PR, Read AJ, Poblete J, et al. TRPA1 Mediates the Inflammatory Actions of Environmental Irritants and Proalgesic Agents. *Cell*. 2006; 124(6):1269–82. <https://doi.org/10.1016/j.cell.2006.02.023> PMID: 16564016
33. Caterina MJ, Leffler A, Malmberg AB, Martin WJ, Trafton J, Petersers-Zeitze KR, et al. Impaired nociception and pain sensation in mice lacking the capsaicin receptor. *Science*. 2000; 288(5464):306–13. PMID: 10764638
34. Perry SW, Norman JP, Barbieri J, Brown EB, Harris A. Gradient: a Practical Usage Guide. *Biotechniques*. 2011; 50(2):98–115. <https://doi.org/10.2144/000113610> PMID: 21486251
35. Ogawa N, Kurokawa T, Mori Y. Sensing of redox status by TRP channels. *Cell Calcium*. 2016; 60(2):115–22. <https://doi.org/10.1016/j.ceca.2016.02.009> PMID: 26969190
36. Gold MS, Gebhart GF. Nociceptor sensitization in pain pathogenesis. *Nat Med*. 2010; 16(11):1248–57. <https://doi.org/10.1038/nm.2235> PMID: 20948530
37. Tatar M, Webber SE, Widdicombe JG. Lung C-fibre receptor activation and defensive reflexes in anaesthetized cats. *J Physiol*. 1988; 402(1):411–20.

38. Morrison SF. Differential control of sympathetic outflow. *Am J Physiol Regul Integr Comp Physiol*. 2001; 281:R689–98.
39. Taylor-Clark TE, Udem BJ, Macglashan DW, Ghatta S, Carr MJ, McAlexander MA. Prostaglandin-induced activation of nociceptive neurons via direct interaction with transient receptor potential A1 (TRPA1). *Mol Pharmacol*. 2008; 73(2):274–81. <https://doi.org/10.1124/mol.107.040832> PMID: 18000030
40. Lai B, Zhang L, Dong LY, Zhu YH, Sun FY, Zheng P. Inhibition of Qi site of mitochondrial complex III with antimycin A decreases persistent and transient sodium currents via reactive oxygen species and protein kinase C in rat hippocampal CA1 cells. *Exp Neurol*. 2005; 194(2):484–94. <https://doi.org/10.1016/j.expneurol.2005.03.005> PMID: 16022873
41. Han D, Williams E, Cadenas E. Mitochondrial respiratory chain-dependent generation of superoxide and its release into the intermembrane space. *Biochem J*. 2001; 353(2):411–6.
42. Chen Q, Vazquez EJ, Moghaddas S, Hoppel CL, Lesnefsky EJ. Production of reactive oxygen species by mitochondria. *J Biol Chem*. 2003; 278(38):36027–31. <https://doi.org/10.1074/jbc.M304854200> PMID: 12840017
43. Turrens JF. Mitochondrial formation of reactive oxygen species. *J Physiol*. 2003; 552(2):335–44.
44. Stowe DF, Camara AKS. Mitochondrial reactive oxygen species production in excitable cells: Modulators of Mitochondrial and Cell Function. *Antioxid Redox Signal*. 2009; 11(6):1373–414. <https://doi.org/10.1089/ARS.2008.2331> PMID: 19187004
45. Gouin O, L'Herondelle K, Lebonvallet N, Le Gall-Ianotto C, Sakka M, Buhé V, et al. TRPV1 and TRPA1 in cutaneous neurogenic and chronic inflammation: pro-inflammatory response induced by their activation and their sensitization. *Protein Cell*. 2017; 8(9):644–61. <https://doi.org/10.1007/s13238-017-0395-5> PMID: 28364279
46. Watanabe H, Vriens J, Prenen J, Groogmans G, Voets T, Nilius B. Anandamide and arachidonic acid use epoxyeicosatrienoic acids to activate TRPV4 channels. *Nature*. 2003; 424(7):434–8.
47. Wen H, Östman J, Bubb KJ, Panayiotou C, Priestley J V, Baker MD, et al. 20-hydroxyeicosatetraenoic acid (20-HETE) is a novel activator of transient receptor potential vanilloid 1 (TRPV1). *J Biol Chem*. 2012; 287(17):13868–76. <https://doi.org/10.1074/jbc.M111.334896> PMID: 22389490
48. Prescott ED, Julius D. A Modular PIP₂ Binding Site as a Determinant of Capsaicin Receptor Sensitivity. *Science*. 2003; 300(5623):1284–8. <https://doi.org/10.1126/science.1083646> PMID: 12764195
49. Votyakova T V, Reynolds IJ. $\Delta\Psi_m$ -Dependent and -independent production of reactive oxygen species by rat brain mitochondria. *J Neurochem*. 2001; 79:266–77. PMID: 11677254
50. Suski JM, Lebiezinska M, Bonora M, Pinton P, Duszynski J, Wieckowski MR. Relation between mitochondrial membrane potential and ROS formation. In: *Methods in Molecular Biology*. 2012. p. 183–205.
51. Sipos I, Tretter L, Adam-Vizi V. The production of reactive oxygen species in intact isolated nerve terminals is independent of the mitochondrial membrane potential. *Neurochem Res*. 2003; 28(10):1575–81. PMID: 14570403
52. Hoffman DL, Brookes PS. Oxygen sensitivity of mitochondrial reactive oxygen species generation depends on metabolic conditions. *J Biol Chem*. 2009; 284(24):16236–45. <https://doi.org/10.1074/jbc.M809512200> PMID: 19366681
53. St-Pierre J, Buckingham JA, Roebuck SJ, Brand MD. Topology of Superoxide Production from Different Sites in the Mitochondrial Electron Transport Chain. *J Biol Chem*. 2002; 277(47):44784–90. <https://doi.org/10.1074/jbc.M207217200> PMID: 12237311
54. Muller FL, Liu Y, Van Remmen H. Complex III releases superoxide to both sides of the inner mitochondrial membrane. *J Biol*. 2004; 279(47):49064–73.
55. Lejen T, Albillos A, Ros SD. Mitochondrial calcium sequestration and protein kinase C cooperate in the regulation of cortical F-actin disassembly and secretion in bovine chromaffin cells. *J Physiol*. 2004; 560(Pt 1):63–76. <https://doi.org/10.1113/jphysiol.2004.064063> PMID: 15133064
56. Rizzuto R, De Stefani D, Raffaello A, Mammucari C. Mitochondria as sensors and regulators of calcium signalling. *Nat Rev Mol Cell Biol*. 2012; 13(9):566–78. <https://doi.org/10.1038/nrm3412> PMID: 22850819
57. Cao E, Cordero-Morales JF, Liu B, Qin F, Julius D. TRPV1 channels are Intrinsically heat sensitive and negatively regulated by phosphoinositide lipids. *Neuron*. 2013; 77(4):667–79. <https://doi.org/10.1016/j.neuron.2012.12.016> PMID: 23439120
58. Mandadi S, Tominaga T, Numazaki M, Murayama N, Saito N, Armati PJ, et al. Increased sensitivity of desensitized TRPV1 by PMA occurs through PKC ϵ -mediated phosphorylation at S800. *Pain*. 2006; 123(1–2):106–16. <https://doi.org/10.1016/j.pain.2006.02.016> PMID: 16564619

59. Bandell M, Story GM, Hwang SW, Viswanath V, Eid SR, Petrus MJ, et al. Noxious cold ion channel TRPA1 is activated by pungent compounds and bradykinin. *Neuron*. 2004; 41(6):849–57. PMID: [15046718](https://pubmed.ncbi.nlm.nih.gov/15046718/)
60. Shishkin V, Potapenko E, Kostyuk E, Girnyk O, Voitenko N, Kostyuk P. Role of mitochondria in intracellular calcium signaling in primary and secondary sensory neurones of rats. *Cell Calcium*. 2002; 32(3):121–30. PMID: [12208232](https://pubmed.ncbi.nlm.nih.gov/12208232/)
61. Wang YY, Chang RB, Waters HN, McKemy DD, Liman ER. The nociceptor ion channel TRPA1 is potentiated and inactivated by permeating calcium ions. *J Biol Chem*. 2008; 283(47):32691–703. <https://doi.org/10.1074/jbc.M803568200> PMID: [18775987](https://pubmed.ncbi.nlm.nih.gov/18775987/)
62. Rohacs T. Phosphoinositide regulation of TRPV1 revisited. *Pflugers Arch Eur J Physiol*. 2015; 467(9):1851–69.
63. Susankova K, Tousova K, Vyklicky L, Teisinger J, Vlachova V. Reducing and Oxidizing Agents Sensitize Heat-Activated Vanilloid Receptor (TRPV1) *Current. Mol Pharmacol*. 2006; 70(1):383–94. <https://doi.org/10.1124/mol.106.023069> PMID: [16614139](https://pubmed.ncbi.nlm.nih.gov/16614139/)
64. Meents JE, Fischer MJM, McNaughton PA. Sensitization of TRPA1 by Protein Kinase A. *PLoS One*. 2017; 12(1):1–15.
65. Weng HJ, Patel KN, Jeske NA, Bierbower SM, Zou W, Tiwari V, et al. Tmem100 Is a regulator of TRPA1-TRPV1 complex and contributes to persistent pain. *Neuron*. 2015; 85(4):833–46. <https://doi.org/10.1016/j.neuron.2014.12.065> PMID: [25640077](https://pubmed.ncbi.nlm.nih.gov/25640077/)
66. Spahn V, Stein C, Zollner C. Modulation of transient receptor vanilloid 1 activity by transient receptor potential ankyrin 1. *Mol Pharmacol*. 2014; 85(2):335–44. <https://doi.org/10.1124/mol.113.088997> PMID: [24275229](https://pubmed.ncbi.nlm.nih.gov/24275229/)